Lucite cuvettes in the dark and stored at 77 K. All subsequent sample handling was done in the dark. Biological activity was measured using a Clark-type O_2 electrode in an assay mixture containing 10 mM $CaCl_2$, 50 mM MES (pH 6), and 0.31 mM 2,6-dichloro-*p*-benzoquinone as an acceptor.

X-ray absorption data were measured at the Stanford Synchrotron Radiation Laboratory (SSRL) wiggler beam line 7-3 under dedicated conditions (3.0 GeV, 40 mA) using a Si(220) double-crystal monochromator detuned 50% for harmonic rejection. Samples were maintained at 10 K using a liquid He flow cryostat, and data were measured as fluorescence excitation spectra using a 13-element Ge detector array. Spectra were calibrated by simultaneously recording the absorption spectrum of $KMnO_4$, with the $KMnO_4$ preedge peak defined as 6543.3 eV. Data were reduced and normalized as previously described.[14] Normalized XANES spectra were fit to linear combinations of spectra drawn from a library of Mn(II), Mn(III), and Mn(IV) reference compounds for quantitative analysis of Mn(II) content.[15]

The OEC XANES spectra are shown in Figure 1. Dark treatment with either reductant generates a new species whose XANES spectrum is consistent with reduction of Mn. Since the changes in the XANES are completely reversed by illumination, they do not result from irreversible damage. This is consistent with there being only small activity losses (0–20%) following the treatments.

We have previously noted[15] the difficulty in determining the relative amounts of Mn(III) and Mn(IV) due to the similarity of their XANES spectra. In contrast, the unique XANES spectra observed for Mn(II) make it relatively easy to quantitate.[16] The results of quantitative fits to the XANES spectra are summarized in Table I. We find no evidence for Mn(II) in the control (S_1) sample. Our previous suggestion[14] that S_1 contains ca. 25% Mn(II) was due to Mn(II) contamination present in the Mylar windows covering those samples.[18] Quantitative comparisons of the fluorescence intensities for Mylar alone and for Mylar-covered OEC samples show that Mn contamination accounted for ca. 25% of the fluorescence intensity, thus confirming the accuracy of our quantitation method. The present samples, measured using Mn-free polypropylene windows, show <5% Mn(II), consistent with the results of Klein, Sauer, and co-workers.[10]

In contrast to the spectra for S_1, the XANES spectra for hydroquinone-treated samples can be fit only by including ca. 30% of a Mn(II) component. This is consistent with the recent observation[19] that a photoreversible Mn(II) six-line EPR signal is produced by hydroquinone treatment. The apparent amount of Mn(II) depends on the oxidation state that is assumed for the remainder of the Mn. The XANES spectra for NH_2OH-treated samples also show reduction relative to S_1. In this case, however, the data can be fit equally well by Mn(III) plus small amounts of either Mn(II) or Mn(IV) or by a ca. 1:3 mixture of Mn(II) and Mn(IV). Regardless of which model is assumed, the edge fitting confirms the reduction of Mn,[16] as expected for the observed shift in edge energy.

The reduction of Mn by hydroxylamine treatment in the dark conflicts with the conclusions of Guiles et al.[10] The difference may be due to the use of different sample preparations (the reaction center complex lacks extrinsic polypeptides and is hence more susceptible to reduction). Alternatively, the difference may lie in the interpretation of the data. The edge shift that we observe is similar to that reported by Guiles et al.[10] In the earlier experiments, this shift was attributed to the formation of inactive centers based on the observation of a Mn(II) EPR signal. As noted above, however, a Mn(II) EPR signal is not necessarily associated with inactive centers.[19] Since we observe little loss of activity and since the treatments are reversible, the reduction observed in our samples cannot be due to inactive centers (the 0–20% centers that are inactivated lose Mn(II) into the supernatant, where it does not contaminate the XANES spectrum). Experiments to resolve the origin of the difference between our conclusions and those of Guiles et al. are in progress.

Figure 1 and Table I show that significantly less Mn(II) is produced by NH_2OH than by hydroquinone. Perhaps this is not surprising considering the higher concentration and longer incubation time used for hydroquinone. However, these reaction conditions were chosen to maximize reductant concentration and exposure time without compromising activity. It is possible to generate a NH_2OH-reduced species with a XANES spectrum identical to that of hydroquinone (not shown); however, such a sample is inactive. This shows that the NH_2OH sample presented here is not simply a mixture of ca. 50% S_1 and 50% of the more reduced derivative formed by hydroquinone.

In a series of reactivity studies,[11,19] Mei and Yocum have shown that hydroxylamine and hydroquinone attack different sites in the OEC. Hydroxylamine-treated samples are EDTA sensitive,[11] but hydroquinone-treated samples are not.[19] There is a strong synergism in the ability of NH_2OH and hydroquinone to inactivate the OEC.[19] It is intriguing that the hydroquinone sensitive site gives more Mn(II) but is not susceptible to EDTA while the NH_2OH sensitive site gives less Mn(II) but is EDTA susceptible. This suggests that NH_2OH may be attacking a water-accessible Mn while hydroquinone reduces Mn that remains sequestered within the protein.

Acknowledgment. Supported in part by grants from the NIH (GM-38047 to J.P.-H. and a Molecular Biophysics Training Grant to P.J.R.) and the USDA, Competitive Research Grants Office, Photosynthesis Program (88-37130-3546 to C.F.Y.). The SSRL is supported by the U.S. DOE and by an NIH Research Resource Grant.

(14) Penner-Hahn, J. E.; Fronko, R. M.; Pecoraro, V. L.; Yocum, C. F.; Betts, S. D.; Bowlby, N. R. *J. Am. Chem. Soc.* **1990**, *112*, 2549–2557.
(15) (a) Waldo, G. S. Ph.D. Thesis, University of Michigan, 1991. (b) Waldo, G. S.; Penner-Hahn, J. E. Manuscript in preparation.
(16) This quantitation procedure assigns all of the XANES changes to oxidation-state changes. XANES *energies* depend somewhat on ligation type;[17] however, in 50 models examined to date, the XANES *shape* for Mn(II) appears to be a unique oxidation-state marker. It should be noted, however, that a hypothetical Mn(III) complex having a Mn(II)-like structure (e.g., Mn–O distances of ca. 2.2 Å) might give changes similar to those in Figure 1.
(17) Kirby, J. A.; Goodin, D. B.; Wydrzynski, T.; Robertson, A. S.; Klein, M. P. *J. Am. Chem. Soc.* **1981**, *103*, 5537–5542.
(18) Waldo, G. S.; Penner-Hahn, J. E. Unpublished results.
(19) Mei, R.; Yocum, C. F. *Biochemistry* **1992**, *31*, 8449–8454.

Long-Range Heteronuclear Spin Locking (HSL) 2D-NMR Spectroscopy and Its Application to the Resonance Assignments of Poly(*p*-*tert*-butylstyrene)

Peter L. Rinaldi,*,† Maritherese Tokles,† Gerard S. Hatvany,† and H. James Harwood‡

Department of Chemistry, Knight Chemical Laboratory, and Department of Polymer Science
The University of Akron, Akron, Ohio 44325-3601

Received July 18, 1992

In this paper, it is demonstrated that heteronuclear spin locking (HSL) 2D-NMR spectroscopy can be used to obtain correlations due to long-range heteronuclear interactions in organic structures, by unequivocally assigning the aromatic ^1H and ^{13}C resonances of isotactic poly(*p*-*tert*-butylstyrene), **1**.

The NMR resonances from the aromatic protons of styrene units in polymers can provide information about stereosequence and monomer unit distributions, but their chemical shift behavior is imperfectly understood. A better understanding of the aromatic resonance patterns of polymers develops concurrently with the understanding of other spectroscopic characteristics of the polymers. Isotactic **1** is a particularly good material to investigate from this standpoint because of its unusually high solubility in common solvents at ambient temperatures, despite its high

† Department of Chemistry.
‡ Department of Polymer Science.

0002-7863/92/1514-10651$03.00/0

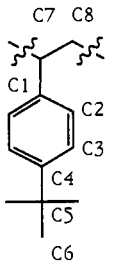

1

stereoregularity. Resonance assignments for **1** will aid subsequent fluorescence studies, and ^1H and ^{13}C NMR studies will explore conformation-related interactions that occur in this polymer.[1]

Chemical shift correlations between ^{13}C and directly bound ^1H are routinely accomplished using HETCOR[2-4] or HMQC.[5,6] However, experiments such as long-range HETCOR,[7] COLOC,[8,9] SINEPT,[10,11] HMBC,[12] and HOESY,[13-15] which utilize long-range J couplings or nuclear Overhauser effects (NOEs), are ineffective with large molecules due to relaxation during the long delays required for internuclear information exchange or the disappearance of NOEs when the molecular tumbling rate approaches the spectrometer frequency. Recent attempts to exploit the sensitivity advantages of state-of-the-art high-field spectrometers have been hampered by these factors and the additional complication that effective chemical shift anisotropy (CSA) contributes to further line broadening. Attempts to obtain COLOC and HOESY spectra of **1** failed for these reasons.[16]

Homonuclear spin locking experiments such as TOCSY and CAMELSPIN/ROESY[17-19] circumvent similar problems associated with the COSY and NOESY[20] experiments. HSL experiments in liquids, first described by Bertrand[21] for cross polarization via one-bond couplings, can be similarly employed to obtain long-range heteronuclear correlations. Their pulse sequence adapted for 2D-HSL is

$$\text{relaxation delay}-90°_x(\text{H})-\frac{t_1}{2}-180°_x(\text{X})-\frac{t_1}{2}-\text{spinlock(H,X)}-\text{decouple(H)},\text{acquire(X)}$$

Cross polarization between ^1H and X nuclei requires satisfaction of the Hartmann–Hahn matching condition $\gamma_H B_2 = \gamma_X B_1$ during the spin locking period, where γ_X and γ_H are magnetogyric ratios of X and H, and B_1 and B_2 are the rf fields of X and H transmitters, respectively. This match is nominally obtained by adjusting the relative powers of the transmitters. However, standard liquid state NMR probes contain separate orthogonal coils to produce the two rf fields, resulting in a nonidentical match over most of the sample, and long mixing times exacerbate field offset effects. Recently it has been shown that efficient heteronuclear J cross polarization in liquids can be achieved by using a multipulse mixing sequence and large spin locking fields.[22-28] In this work, combined use of MLEV-17[29] spin locking and a special probe in which one coil is doubly tuned for the ^1H and X frequencies provides identical B_1 and B_2 fields over the entire active coil volume for all the spins of interest.

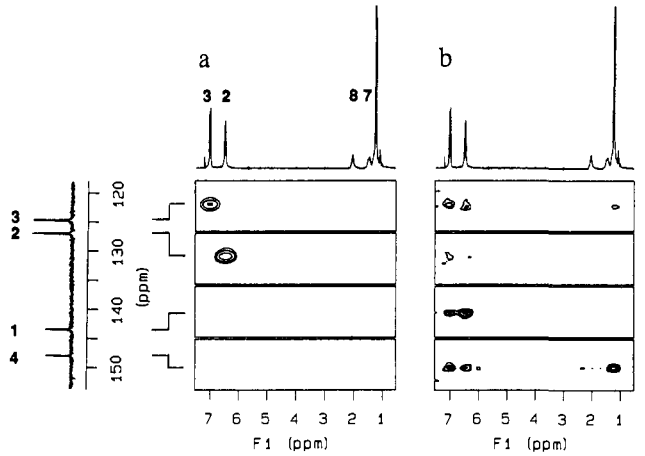

Figure 1. Phase-sensitive HSL spectra of isotactic poly(*p-tert*-butylstyrene) (MW = 260 000, 0.150 g in 0.5 mL of $CDCl_3$ contained in a 5-mm sample tube at 50 °C) observed at 75.4 MHz and utilizing two mix times, (a) 10 ms and (b) 300 ms. The data were acquired as follows: f_2-dimension 2700-Hz spectral window, 2048 points, 1-s relaxation delay, 20.5-μs 90° ^{13}C pulse width, and 764 transients/FID; f_1-dimension 13.5-μs 90° ^1H pulse width, 64 FIDs with the evolution time incremented to provide a 3000-Hz spectral window. The transmitters were placed at 4.0 and 136 ppm in the ^1H and ^{13}C dimensions, respectively. Synchronous ^1H and ^{13}C MLEV-17 multipulse decoupling was used for spin locking with $\gamma B_1/2\pi = \gamma B_2/2\pi = 3$ kHz. The ^1H transmitter was set in the middle of the ^1H spectral window. Phase cycling was performed according to the method described by States et al.[31] The total experiment time was 18 h/spectrum. A hypercomplex FT was performed on the 4096 × 1024 matrix with shifted sine-bell weighting. Spectra are presented in absolute value mode with the same relative vertical scaling factors and with contour spacing of 1.5. The 1D NMR spectra are placed along the appropriate axes, along with numbering corresponding to the resonance assignments.

Two HSL experiments with mixing times of 10 and 300 ms, shown in parts a and b, respectively, of Figure 1, permit the complete aromatic ^1H and ^{13}C resonance assignments of **1**.[30] Figure 1a exhibits only one-bond correlations between ^1H and ^{13}C, arising predominantly from $^1J_{CH}$ interactions.

At the longer mixing times (Figure 1b), additional cross peaks appear as a consequence of longer range interactions. These cross

(1) Chakraborty, D. K.; Heitzhaus, K. D.; Hamilton, F. J.; Harwood, H. J.; Mattice, W. L. *Macromolecules* **1991**, *24*, 75.
(2) Maudsley, A. A.; Muller, L.; Ernst, R. R. *J. Magn. Reson.* **1977**, *28*, 463.
(3) Bodenhausen, G.; Freeman, R. *J. Magn. Reson.* **1977**, *28*, 471.
(4) Freeman, R.; Morris, G. A. *J. Chem. Soc., Chem. Commun.* **1978**, 684.
(5) Muller, L. *J. Am. Chem. Soc.* **1979**, *101*, 4481.
(6) Bax, A.; Griffey, R. H.; Hawkins, B. L. *J. Magn. Reson.* **1983**, *55*, 301.
(7) Hallenga, K.; Binst, G. V. *Bull. Magn. Reson.* **1980**, *2*, 343.
(8) Kessler, H.; Griesinger, C.; Zarbock, J.; Loosli, H. R. *J. Magn. Reson.* **1984**, *57*, 331.
(9) Kessler, H.; Bermel, W.; Griesinger, C. *J. Am. Chem. Soc.* **1985**, *107*, 1083.
(10) Bax, A. *J. Magn. Reson.* **1984**, *57*, 314.
(11) Nielson, N. C.; Bildsoe, H.; Jakobsen, H. J.; Sorensen, O. W. *J. Magn. Reson.* **1986**, *66*, 456.
(12) Bax, A.; Summers, M. F. *J. Am. Chem. Soc.* **1986**, *108*, 2093.
(13) Rinaldi, P. L. *J. Am. Chem. Soc.* **1983**, *105*, 5167.
(14) Yu, C.; Levy, G. C. *J. Am. Chem. Soc.* **1983**, *105*, 6994.
(15) Kover, K. E.; Batta, G. *Prog. Nucl. Magn. Reson. Spectrosc.* **1987**, *19*, 223.
(16) Literature values for long-range C–H J couplings in molecules similar to poly(*p-tert*-butylstyrene) could not be found, and these values could not be determined from the polymer itself. We have measured J couplings from ^{13}C NMR spectra of 4-*tert*-butylphenol (0.4 g in 0.7 mL of $CDCl_3$) with selective decoupling of the *tert*-butyl ^1H resonance: $^2J_{C2\text{-}H3} = 5.0$ Hz; $^2J_{C3\text{-}H2} = 7.8$ Hz; $^2J_{C4\text{-}H3} = 6.7$ Hz; $^2J_{C1\text{-}H2} = 9.5$ Hz; $^3J_{C4\text{-}H2} = 2.5$ Hz.
(17) Bothner-By, A. A.; Stephens, R. L.; Lee, J. T.; Warren, C. D.; Jeanloz, R. W. *J. Am. Chem. Soc.* **1984**, *106*, 811.
(18) Bax, A.; Davis, D. G. *J. Magn. Reson.* **1985**, *63*, 207.
(19) Davis, D. G.; Bax, A. *J. Am. Chem. Soc.* **1985**, *107*, 2820.
(20) Macura, S.; Ernst, R. R. *Mol. Phys.* **1980**, *41*, 95.
(21) Bertrand, R. D.; Moniz, W. B.; Garroway, A. N.; Chingas, G. C. *J. Am. Chem. Soc.* **1978**, *100*, 5227.
(22) Bearden, D. W.; Brown, L. R. *Chem. Phys. Lett.* **1989**, *163*, 432.
(23) Zuiderweg, E. R. P. *J. Magn. Reson.* **1990**, *89*, 533.
(24) Kellogg, G. W. *J. Magn. Reson.* **1992**, *97*, 623.
(25) Artemov, D. Y. *J. Magn. Reson.* **1991**, *91*, 405.
(26) Brown, L. R.; Sanctuary, B. C. *J. Magn. Reson.* **1991**, *91*, 413.
(27) Morris, G. A.; Gibbs, A. *J. Magn. Reson.* **1991**, *91*, 444.
(28) Nuzillard, J. M.; Massiot, G. *J. Magn. Reson.* **1991**, *91*, 380.
(29) Levitt, M. H.; Freeman, R.; Frenkiel, R. *J. Magn. Reson.* **1982**, *50*, 157.
(30) The resonance assignments for isotactic poly(*p-tert*-butylstyrene) are as follows: ^{13}C NMR δ (relative to $CDCl_3$ at 77.0) C-1 143.54, C-2 127.11, C-3 124.80, C-4 148.05, C-5 34.24, C-6 31.50, C-7 39.80, C-8 42.86; ^1H NMR δ (relative to $CHCl_3$ at 7.25) H-2 6.47 (d, $J = 7.3$ Hz), H-3 7.01 (d, $J = 7.5$ Hz), H-6 1.23 (s), H-8a 2.03 (m), H-8b and H-7 1.49 (m). The ^{13}C NOEs measured by a gated decoupling experiment are C-1, 1.29; C-2, 1.48; C-3, 1.49; C-4, 1.11; C-5, 2.08; C-6, 2.82; C-7, 1.42; C-8, 1.31.
(31) States, D. J.; Haberkorn, R. A.; Ruben, D. J. *J. Magn. Reson.* **1982**, *48*, 286.

peaks might result from a number of mechanisms involving permutations of *J*-coupling interactions. Cross peaks between the ^{13}C resonances at 124.8 and 148.05 ppm and the *tert*-butyl ^1H resonance identify these as the C-3 and C-4 resonances, respectively. The former cross peak might arise from an initial ROESY transfer from the *tert*-butyl protons to H-3, followed by heteronuclear TOCSY transfer from H-3 to C-3 via one-bond coupling. The latter cross peak might arise from an initial ROESY transfer from the *tert*-butyl protons to H-3, followed by heteronuclear TOCSY transfer from H-3 to C-4 via long-range coupling ($^2J_{H3-C4} \approx 7.0$ Hz).[16] These cross peaks were not detected in other experiments which rely on development of coherence through *J* coupling in the laboratory frame.

HSL provides a valuable means of obtaining long-range structural information in high molecular weight molecules and promises to be an effective means of reducing the problems of rapid CSA relaxation encountered on very high field NMR spectrometers.

Acknowledgment. We thank Kevin D. Heitzhaus for the preparation of the isotactic poly(*p*-*tert*-butylstyrene). This work was supported by funds from a University of Akron Faculty Research Grant, a State of Ohio Board of Regents Academic Challenge Grant, NIH Award R15-GM44409-01, and a grant from the NSF Chemical Instrumentation Program (CHE-8820644).

Registry No. 1, 30998-04-0.

Highly Stereocontrolled Total Synthesis of (+)-Allopumiliotoxin 339A

Sakae Aoyagi, Tzu-Chueh Wang, and Chihiro Kibayashi*

Tokyo College of Pharmacy
Horinouchi, Hachioji
Tokyo 192-03, Japan

Received August 28, 1992

The dendrobatid alkaloids of the allopumiliotoxin A class, a series of the naturally occurring 7-hydroxy congeners of the pumiliotoxin A class, are one of the most structurally complex indolizidines produced in nature.[1] The distinct chemical structure and the significant biological activities of this class of alkaloids[2] have provided the stimulus for development of new methodologies for their syntheses, and two successful approaches to allopumiliotoxins 267A and 339B have been reported by Overman et al.[3a] and Trost et al.[3b] Recently, the first total synthesis of (+)-allopumiliotoxin 339A (**1**), isolated as a minor constituent from skin extracts of a family of Panamanian poison frogs, *Dendrobates auratus*,[4] has been published by Overman's group.[5]

In this communication we report a highly stereocontrolled approach to the synthesis of **1**, which provides an efficient, novel entry to the allopumiliotoxin A alkaloids. Such an approach is based upon intramolecular cyclization of **3** (X = halogen) for the formation of **1** involving direct construction of the 6-(*E*)-alkylideneindolizidine ring system as well as establishing the trans-diaxial 7,8-diol on the indolizidine ring as shown in Scheme I. We envisioned that this process would exploit the intramolecular Cr(II)-mediated coupling reaction[6] originally studied by Nozaki and co-workers,[7] wherein the cyclization would proceed via an alkenylchromium(III) species **2**.

Scheme I

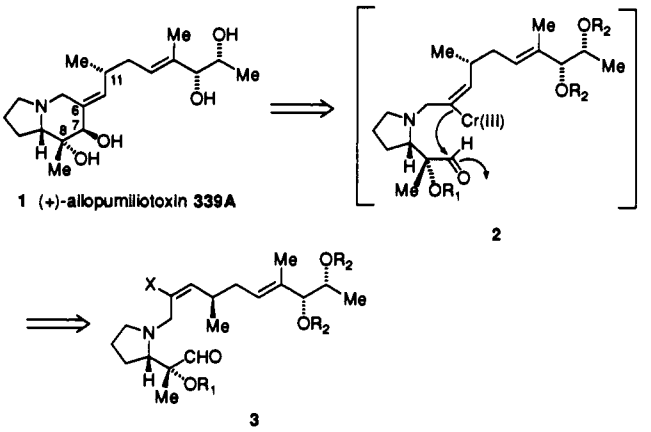

Scheme II[a]

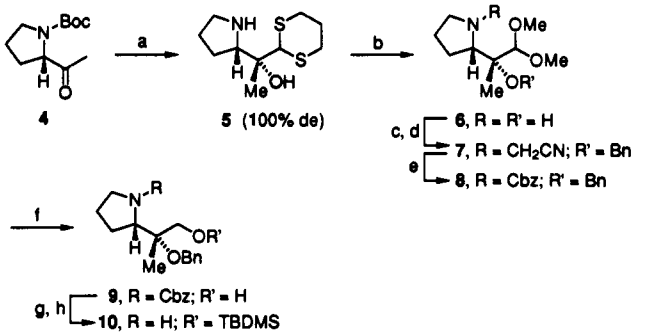

[a] (a) CF_3CO_2H (3 equiv), CH_2Cl_2, room temperature, then 1,3-dithiane (5 equiv), BuLi (5 equiv), THF, −78 °C; (b) MeOH, $Hg(ClO_4)_2 \cdot xH_2O$, $CHCl_3$, room temperature; (c) ICH_2CN, Et_3N, THF, room temperature; (d) BnBr, KH, THF, reflux; (e) $AgNO_3$, EtOH, room temperature, then CbzCl, Et_3N, CH_2Cl_2, room temperature; (f) 3 N HCl, THF, room temperature, then $NaBH_4$, MeOH, room temperature; (g) *t*-$BuMe_2SiCl$, imidazole, DMF, room temperature; (h) H_2, 10% Pd/C, MeOH.

Scheme III[a]

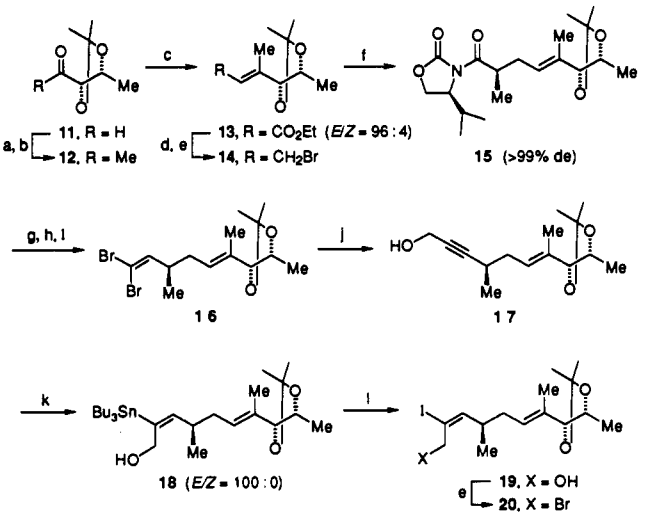

[a] (a) MeMgBr, THF, 0 °C; (b) PCC, CH_2Cl_2, room temperature; (c) $(i\text{-}PrO)_2P(O)CH_2CO_2Et$, NaH, benzene, room temperature; (d) DIBALH, CH_2Cl_2/hexane, −78 °C; (e) CBr_4, PPh_3, CH_2Cl_2, 0 °C; (f) (*S*)-4-isopropyl-3-propionyl-2-oxazolidinone, LDA, THF, 0 °C; (g) $LiAlH_4$, THF, 0 °C; (h) DMSO, $(COCl)_2$, Et_3N, −78 °C; (i) CBr_4 (2 equiv), PPh_3 (4 equiv), CH_2Cl_2, 0 °C; (j) $(CH_2O)_n$, BuLi (2 equiv), THF, room temperature; (k) Bu_3SnH, $PdCl_2(PPh_3)_2$ (2 mol %), THF, room temperature; (l) I_2, CH_2Cl_2, room temperature.

(1) Daly, J. W.; Spande, T. F. In *Alkaloids: Chemical and Biological Perspectives*; Pelletier, S. W., Ed.; Wiley: New York, 1986; Vol. 4, Chapter 1, pp 1-274.
(2) (a) Albuquerque, E. X.; Warnick, J. E.; Maleque, M. A.; Kauffman, F. C.; Tamburini, R.; Nimit, Y.; Daly, J. W. *Mol. Pharmacol.* **1981**, *19*, 411. (b) Daly, J. W.; McNeal, E. T.; Overman, L. E.; Ellison, D. H. *J. Med. Chem.* **1985**, *28*, 482. (c) Daly, J. W.; Gusovsky, F.; McNeal, E. T.; Secunda, S.; Bell, M.; Creveling, C. R.; Nishizawa, Y.; Overman, L. E.; Sharp, M. J.; Rossignol, D. P. *Biochem. Pharmacol.* **1990**, *40*, 315.
(3) (a) Overman, L. E.; Goldstein, S. W. *J. Am. Chem. Soc.* **1984**, *106*, 5360. (b) Trost, B. M.; Scanlan, T. S. *J. Am. Chem. Soc.* **1989**, *111*, 4988.
(4) Tokuyama, T.; Daly, J. W.; Highet, R. J. *Tetrahedron* **1984**, *40*, 1183.
(5) Overman, L. E.; Robinson, L. A.; Zablocki, J. *J. Am. Chem. Soc.* **1992**, *114*, 368.

0002-7863/92/1514-10653$03.00/0